J. Fluid Mech. (1984), *vol.* 147, *pp.* 159–168
Printed in Great Britain

Stability of compressible Ekman boundary-layer flow

By HANS MOBERG,
Alfa-Laval AB, Tumba, Sweden

LENNART S. HULTGREN
Department of Mechanical Engineering, Illinois Institute of Technology, Chicago, IL 60616

AND FRITZ H. BARK
Department of Mechanics, Royal Institute of Technology, Stockholm, Sweden

(Received 6 April 1982 and in revised form 28 February 1984)

The linear stability properties of the Ekman layer in a rapidly rotating gas have been computed numerically. The two types of instability present in an Ekman layer of a homogeneous fluid, which are usually called classes A and B, respectively, are significantly modified by the compressibility. The critical Reynolds number for the class A instability is found to first increase and then decrease for increasing values of the Mach number. The instability waves of class B are monotonically destabilized as the value of the Mach number increases. In addition, a new class of unstable waves appears for a finite value of the Mach number.

1. Introduction

Experiments by Faller (1963), Tatro & Mollo-Christensen (1967) and Caldwell & Van Atta (1970) and numerical calculations by Faller & Kaylor (1966), Lilly (1966) and Spooner & Criminale (1982) show that the Ekman layer in a homogeneous rotating fluid exhibits two types of instability. The stability properties of the incompressible Ekman layer are also discussed in some detail by Greenspan (1968). The experiments indicated that the occurrence of instability depends mainly on local flow conditions. The first type of instability (class A), which has the lowest critical Reynolds number, is induced by the Coriolis force and appears for a Reynolds number of about 56 based on the boundary-layer thickness and the local value of the geostrophic swirl velocity outside of the Ekman layer. The critical Reynolds number for that type of instability increases linearly with the Rossby number. The other type of instability (class B) is essentially an inviscid inflectional instability modified by rotation. The critical Reynolds number for the class B type instability is about 125, and it is virtually independent of the Rossby number. The numerically computed critical Reynolds numbers are in good agreement with the experimental findings. Lilly (1966) found that the two modes of instability appears for Reynolds numbers larger than 55 and 115 respectively. The temporal evolution of a pulse-like initial disturbance has been investigated numerically by Spooner & Criminale (1982); the continuous temporal eigenvalue spectrum has been analysed by Spooner (1982).

Wave motion in the flow outside of the Ekman layers in a rapidly rotating gas has been analysed by Morton & Shaughnessy (1972), Gans (1974, 1975), Warren (1975), Lalas (1975), Hultgren (1978) and Miles (1981).

In the present paper, the effects of compressibility and heat conduction in a rapidly

rotating gas on the stability of the Ekman layer are explored. The stability problem is formulated in §2 and the numerical results are discussed in §3.† The limitation of the analysis, due to the low density, i.e. long mean free path, that is likely to occur in a typical gas centrifuge, is discussed in the Appendix.

2. Formulation

In a frame of reference rotating with the constant angular velocity $\boldsymbol{\Omega}$, the motion of a compressible, viscous and heat-conducting perfect gas is governed by the following equations:

$$\frac{\mathrm{D}\rho^*}{\mathrm{D}t^*} + \rho^* \nabla \cdot \boldsymbol{u}^* = 0, \tag{2.1}$$

$$\rho^* \left[\frac{\mathrm{D}\boldsymbol{u}^*}{\mathrm{D}t^*} + 2\boldsymbol{\Omega} \times (\boldsymbol{\Omega} \times \boldsymbol{r}^*) \right] = -\nabla p^* + \mu \nabla^2 \boldsymbol{u}^* + (\tfrac{1}{3}\mu + \zeta)\, \nabla(\nabla \cdot \boldsymbol{u}^*), \tag{2.2}$$

$$c_p \rho^* \frac{\mathrm{D}T^*}{\mathrm{D}t^*} - \frac{\mathrm{D}p^*}{\mathrm{D}t^*} = \zeta(\nabla \cdot \boldsymbol{u}^*)^2 + \rho^* \Phi + k \nabla^2 T^*, \tag{2.3}$$

$$p^* = \rho^* R T^*. \tag{2.4}$$

Equations (2.1)–(2.3) describe the conservation of mass, linear momentum and energy respectively; (2.4) is the equation of state; ρ^*, $\boldsymbol{u}^*$, p^* and T^* are the density, velocity, pressure and temperature fields respectively; g is the gravitational acceleration; Φ is the rate of dissipation of mechanical energy, per unit mass of the gas (cf. Batchelor 1967, equation (3.4.5)); μ, ζ, c_p, k and R are the dynamic shear viscosity, bulk viscosity, specific heat at constant pressure, thermal conductivity and gas constant respectively; $\mathrm{D}/\mathrm{D}t^*$ is the material derivative.

Consider a gas of constant temperature T^*_∞, which is contained in e.g. a cylindrical vessel with flat top and bottom walls. The walls of the container are assumed to be perfect thermal conductors. The vessel is rotating with the constant angular velocity Ω around its axis of symmetry, which is taken to be the z-axis. Let the bottom of the container be located at $z = 0$. If the gas is rotating rigidly with the vessel and the rotation is sufficiently rapid for effects of gravity to be negligible, (2.1)–(2.4) show that the density field ρ^*_∞ and the pressure field p^*_∞ are given by

$$\rho^*_\infty(r^*) = \rho^*_\infty(r^*_0) \exp\left\{ \frac{\gamma M^2}{2} \left[\left(\frac{r^*}{r^*_0} \right)^2 - 1 \right] \right\}, \tag{2.5}$$

$$p^*_\infty(r^*) = \frac{(r^*_0 \Omega)^2}{\gamma M^2} \rho^*_\infty(r^*), \tag{2.6}$$

where

$r^* \equiv$ distance from the axis of rotation, (2.7a)

$r^*_0 \equiv$ characteristic distance from the axis of rotation, (2.7b)

$\gamma \equiv$ ratio of specific heats at constant pressure and volume, (2.7c)

$$M = \frac{r^*_0 \Omega}{(\gamma R T^*_\infty)^{\frac{1}{2}}} \equiv \text{Mach number at } r^* = r^*_0, \tag{2.7d}$$

By some external means, which need not be specified for the present purpose, the motion of the gas is now made to deviate slightly from rigid-body rotation by a steady axisymmetric geostrophic flow field. In general, an Ekman boundary layer will then be located at the horizontal walls. Based on the geostrophic flow, a Rossby number can be defined as

$$Ro = \frac{V^*_g(r^*_0, 0)}{r^*_0 \Omega}, \tag{2.8}$$

† *Note added in proof*: Spall & Wood (1984) have recently performed similar calculations.

where $V_g^*(r_0^*, 0)$ is the azimuthal velocity component of the geostrophic flow field at the edge of the Ekman layer. The Rossby number is taken to be small. Assuming the geostrophic flow to be known, the following expressions for the flow field inside the Ekman layer can be derived from (2.1)–(2.4) by using linearized theory:

$$u_0^* = -Ro\, r_0^*\, \Omega \left\{ \kappa^2 \mathrm{e}^{-\kappa z^*/r_0^* E^{\frac{1}{2}}} \sin \frac{\kappa z^*}{r_0^* E^{\frac{1}{2}}} + O(E^{\frac{1}{2}}) \right\}, \tag{2.9a}$$

$$v_0^* = Ro\, r_0^*\, \Omega \left\{ 1 - \mathrm{e}^{-\kappa z^*/r_0^* E^{\frac{1}{2}}} \cos \frac{\kappa z^*}{r_0^* E^{\frac{1}{2}}} + O(E^{\frac{1}{2}}) \right\}, \tag{2.9b}$$

$$w_0^* = O(Ro\, r_0^*\, \Omega E^{\frac{1}{2}}), \tag{2.9c}$$

$$p_0^* = -Ro\, \rho_\infty^*(r_0^*)\, (r_0^*\, \Omega)^2 \left[\frac{2(1+\alpha^2)}{\gamma M^2} + O(E) \right], \tag{2.9d}$$

$$\rho_0^* = -2Ro\, \rho_\infty^*(r_0^*) \left\{ 1 + \alpha^2 \mathrm{e}^{-\kappa z^*/r_0^* E^{\frac{1}{2}}} \cos \frac{\kappa z^*}{r_0^* E^{\frac{1}{2}}} + O(E^{\frac{1}{2}}) \right\}, \tag{2.9e}$$

$$T_0^* = -2Ro\, T_\infty^*\, \alpha^2 \left\{ 1 - \mathrm{e}^{-\kappa z^*/r_0^* E^{\frac{1}{2}}} \cos \frac{\kappa z^*}{r_0^* E^{\frac{1}{2}}} + O(E^{\frac{1}{2}}) \right\}. \tag{2.9f}$$

u_0^*, v_0^*, and w_0^* are the velocity components in the radial, azimuthal and axial directions respectively;

$$E = \frac{\mu}{\rho_\infty^*(r_0^*)\, r_0^{*2}\, \Omega} \tag{2.10a}$$

is the Ekman number at $r^* = r_0^*$;

$$\kappa = (1+\alpha^2)^{\frac{1}{4}}, \quad \alpha^2 = \tfrac{1}{4}\sigma(\gamma-1)\, M^2, \tag{2.10b,c}$$

where σ is the Prandtl number of the gas. The Ekman number is taken to be small. The parameter α^2 can be interpreted as a measure of the ratio of the divergence of the heat flux and the rate of compression work in the Ekman layer. Note that the axial velocity component is $O(E^{\frac{1}{2}})$, and therefore does not affect the stability problem to lowest order.

To investigate the stability properties of the laminar Ekman layer, the temporal evolution of small perturbations on the steady flow in this layer will be considered. Suitable definitions for the non-dimensional variables describing the perturbed flow inside the Ekman layer are

$$\boldsymbol{r}^* = r_0^*(\boldsymbol{e}_r + E^{\frac{1}{2}}\boldsymbol{r}), \quad \text{length}, \tag{2.11a}$$

$$t^* = E^{\frac{1}{2}}(Ro\, \Omega)^{-1} t, \quad \text{time}, \tag{2.11b}$$

$$\boldsymbol{u}^* = Ro\, r_0^*\, \Omega(\boldsymbol{u}_0 + \epsilon \boldsymbol{u}), \quad \text{velocity}, \tag{2.11c}$$

$$p^* = \rho_\infty^*(r_0^*)\, (r_0^*\, \Omega)^2\, [p_\infty + Ro(p_0 + \epsilon Ro\, p)], \quad \text{pressure}, \tag{2.11d}$$

$$\rho^* = \rho_\infty^*(r_0^*)\, [\rho_\infty + Ro(\rho_0 + \epsilon\rho)], \quad \text{density}, \tag{2.11e}$$

$$T^* = T_\infty^* [1 + Ro(T_0 + \epsilon T)], \quad \text{temperature}, \tag{2.11f}$$

ρ_∞ and p_∞ are the non-dimensional density and pressure fields respectively of the rigidly rotating gas. Dependent variables denoted by the subscript zero are associated with the steady Ekman layer, and $\boldsymbol{u}$, p, ρ and T are the dependent variables describing the perturbation flow field. $\boldsymbol{e}_r$ is the unit vector in the radial direction. ϵ is a non-dimensional amplitude of the perturbation flow field, and is assumed to be small. There are thus three small non-dimensional parameters in the problem: ϵ, E and Ro. For consistency, i.e. in order to obtain a meaningful perturbation problem, one must

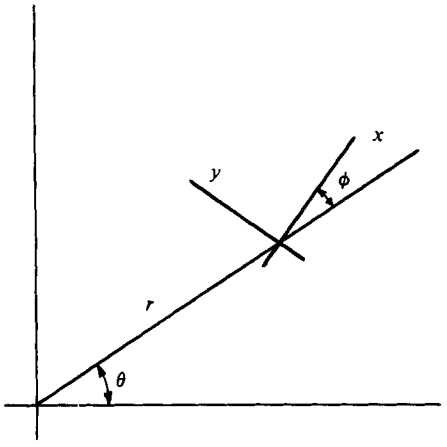

FIGURE 1. Orientation of the local coordinate system.

require that the Reynolds number based on the geostrophic swirl velocity at the edge of the Ekman layer and the local boundary-layer thickness

$$Re = Ro/E^{\frac{1}{2}} \tag{2.12}$$

be finite, however.

The perturbation motion is governed by the following linearized equations:

$$\nabla \cdot \boldsymbol{u} = 0, \tag{2.13}$$

$$Re\left[\frac{\partial \boldsymbol{u}}{\partial t} + (\boldsymbol{u}_0 \cdot \nabla)\,\boldsymbol{u} + \boldsymbol{e}_z \cdot \boldsymbol{u}\frac{\mathrm{d}\boldsymbol{u}_0}{\mathrm{d}z}\right] + 2\boldsymbol{e}_z \times \boldsymbol{u} + \rho \boldsymbol{e}_z \times (\boldsymbol{e}_z \times \boldsymbol{r}) = -Re\,\nabla p + \nabla^2 \boldsymbol{u}, \tag{2.14}$$

$$\sigma Re\left[\frac{\partial T}{\partial t} + (\boldsymbol{u}_0 \cdot \nabla)\,T + \boldsymbol{e}_z \cdot \boldsymbol{u}\frac{\mathrm{d}T_0}{\mathrm{d}z}\right] - 4\alpha^2 \boldsymbol{e}_r \cdot \boldsymbol{u} = \nabla^2 T, \tag{2.15}$$

$$\rho + T = 0, \tag{2.16}$$

where only the leading-order terms in the Rossby number have been retained. $\boldsymbol{e}_z$ is the unit vector in the axial direction. Because of the term $-4\alpha^2 \boldsymbol{e}_r \cdot \boldsymbol{u}$ in (2.15), which represents the rate of compression work, the set of equations (2.13)–(2.16) does not constitute a local Boussinesq-type approximation.

The set of equations (2.13)–(2.16) will be analysed by using the method of normal modes. The continuous spectrum will not be addressed here, however. It is of advantage to introduce a new local coordinate system aligned with the wave fronts of the disturbances (cf. figure 1). The local x-coordinate is in the normal direction, and the local y-coordinate measures distance along the wave front. New mean and perturbation variables are defined as follows:

$$U = u_0 \cos\phi + v_0 \sin\phi, \quad V = -u_0 \sin\phi + v_0 \cos\phi, \tag{2.17a,b}$$

$$\tilde{u} = u \cos\phi + v \sin\phi, \quad \tilde{v} = -u \sin\phi + v \cos\phi, \quad \tilde{w} = w, \tag{2.17c,d,e}$$

where ϕ is the orientation angle defined by the local x-axis and the radial direction (see figure 1). Because the perturbation quantities are independent of the y-coordinate, a stream function ψ can be defined as

$$\tilde{u} = \frac{\partial \psi}{\partial z}, \quad \tilde{w} = -\frac{\partial \psi}{\partial x}. \tag{2.18a,b}$$

Application of the normal-mode assumption, i.e.

$$\begin{bmatrix} \psi \\ \tilde{v} \\ T \end{bmatrix} = \begin{bmatrix} \hat{\psi}(z) \\ \hat{v}(z) \\ \hat{T}(z) \end{bmatrix} e^{ik(x-ct)}, \tag{2.19}$$

leads after some algebraic manipulations to the following set of coupled ordinary differential equations for the perturbation quantities:

$$\hat{\psi}^{iv} - 2k^2\hat{\psi}'' + k^4\hat{\psi} - ik\,Re[(U-c)(\hat{\psi}'' - k^2\hat{\psi}) - U''\hat{\psi}] + 2\hat{v}' - \hat{T}'\cos\phi = 0, \tag{2.20}$$

$$\hat{v}'' - k^2\hat{v} - ik\,Re[(U-c)\hat{v} - V'\hat{\psi}] - 2\hat{\psi}' + \hat{T}\sin\phi = 0, \tag{2.21}$$

$$\hat{T}'' - k^2\hat{T} - i\sigma k\,Re[(U-c)\hat{T} - T_0'\hat{\psi}] + 4\alpha^2(\hat{\psi}'\cos\phi - \hat{v}\sin\phi) = 0, \tag{2.22}$$

where k is the wavenumber, which is taken to be real, and $c = c_r + ic_i$ is the complex phase velocity; kc_i is the growth rate. The prime denotes differentiation with respect to the axial coordinate. Equations (2.20)–(2.22) are to be solved subject to the boundary conditions

$$\hat{\psi} = \hat{\psi}' = \hat{v} = \hat{T} = 0 \quad \text{on} \quad z = 0, \qquad (\hat{\psi}, \hat{\psi}', \hat{v}, \hat{T}) \to 0 \quad \text{as} \quad z \to +\infty. \tag{2.23a, b}$$

For given values of the parameters σ, α^2, Re, k and ϕ, the set (2.20)–(2.22) and the boundary conditions (2.23) define an eigenvalue problem for the complex wave speed c. The laminar flow field is linearly unstable for a given parameter combination if at least one eigenmode has kc_i greater than zero. The critical Reynolds number for linear instability of the compressible boundary layer flow depends, in addition to the wavenumber k and the angle of orientation ϕ on the compressibility and the heat conduction through the parameters α^2 and σ respectively, i.e.

$$Re_c = Re_c(k, \sigma, \alpha^2, \phi). \tag{2.24}$$

Note that all the effects of compressibility are described by the single parameter α^2. This is in contrast with the stability problem for compressible non-rotating parallel shear flows where γ and M must both be specified (Lin 1966).

As can be seen from (2.9) and (2.20)–(2.23), the temperature field decouples from the velocity field in the limit of α^2 tending to zero, i.e. the stability problem for an Ekman layer in a homogeneous fluid is recovered. This limit also includes the case of a heavy gas, i.e. $\gamma - 1 \ll 1$, if the Mach number is of order unity. The heavy-gas limit is not uniformly valid for large Mach numbers, however.

3. Results

The eigenvalues of the problem defined by (2.20)–(2.23) were determined numerically. Starting values for the numerical procedure were obtained from asymptotic solutions valid in the limit of z tending to infinity. A Runge–Kutta scheme was used to numerically integrate the differential equations towards the wall. Orthogonalization of the solution vectors was performed whenever deemed necessary to preserve their linear independence. The eigenvalues were determined to three decimal places. Eigenvalues and critical Reynolds numbers obtained for $\alpha^2 = 0$ were compared with the results for the incompressible case presented by Lilly (1966), Nielsen & True (1978) and Gusev & Bark (1980), and good agreement was demonstrated. The details of the numerical procedure are given in Moberg (1979).

Numerical calculations for finite values of the compressibility parameter, α^2, are shown in figures 2–5. The values of γ and σ are those for air at room temperature,

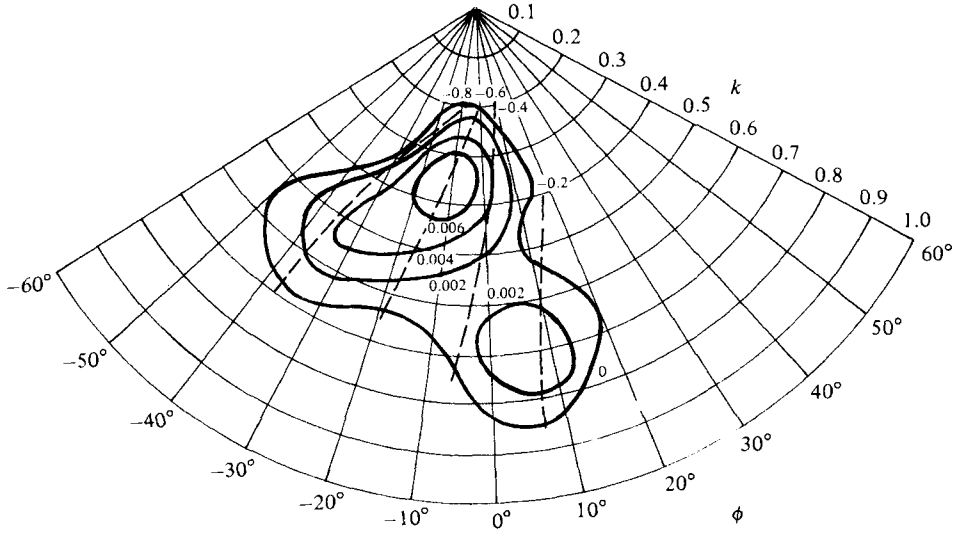

FIGURE 2. Growth rates kc_i (solid curves) and phase velocities c_r (dashed curves) of the most unstable mode as functions of the wavenumber k and orientation angle ϕ. $M = 5$ and $Re = 90$.

		Class A			Class B			Class C		
M	α^2	Re_c	k_c	ϕ_c	Re_c	k_c	ϕ_c	Re_c	k_c	ϕ_c
0	0.000	54.1	0.32	−23°	112.7	0.55	7°	—	—	—
2	0.288	60.9	0.32	−19°	105.3	0.58	7°	—	—	—
5	1.800	66.3	0.37	−11°	85.7	0.69	6°	—	—	—
8	4.608	61.1	0.44	−8°	71.7	0.81	4°	61.5	0.69	−40°
12	10.368	53.3	0.52	−5°	59.6	0.95	3°	52.0	0.85	−43°

TABLE 1. Critical Reynolds number, and corresponding wavenumber and orientation angle, as functions of the Mach number for air at room temperature

i.e. $\gamma = 1.40$ and $\sigma = 0.72$. As in the homogeneous-fluid case, it was found that more than one unstable region may exist in the (k, ϕ)-plane for given values of Re and α^2. These regions correspond to distinct modes of instability. Figure 2 shows the phase velocities and growth rates of the instability modes at a Mach number equal to five and a Reynolds number of 90. The two types of instability modes, commonly labelled class A and class B, found in the homogeneous fluid case (Lilly 1966) are also present here. The class A instability modes are characterized by phase velocities of order unity and small negative angles of orientation. The class B modes have low phase velocities and small positive angles of orientation. As can be seen in table 1, the critical Reynolds number for class A type instability is, for these values of α^2 and σ, higher than the one for the incompressible case. Also, the compressibility and the heat conductivity tend to destabilize class B modes. For increasing values of α^2, the critical Reynolds number decreases and, for a fixed Reynolds number, the growth rate increases. As can be seen in figure 3, where the Mach number is the same as in figure 2 but the Reynolds number equals 150, the class B modes are clearly more unstable than the class A modes. For a homogeneous fluid (Lilly 1966), the growth rates of the two modes are of about equal magnitude at this Reynolds number.

As the Mach number is increased, a new type of instability can be observed (see

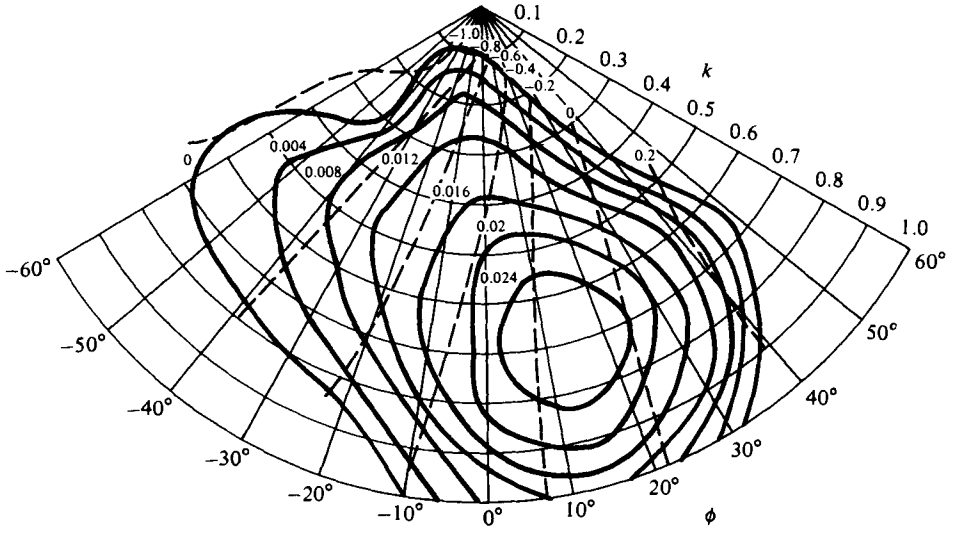

FIGURE 3. Same as figure 2 except $Re = 150$.

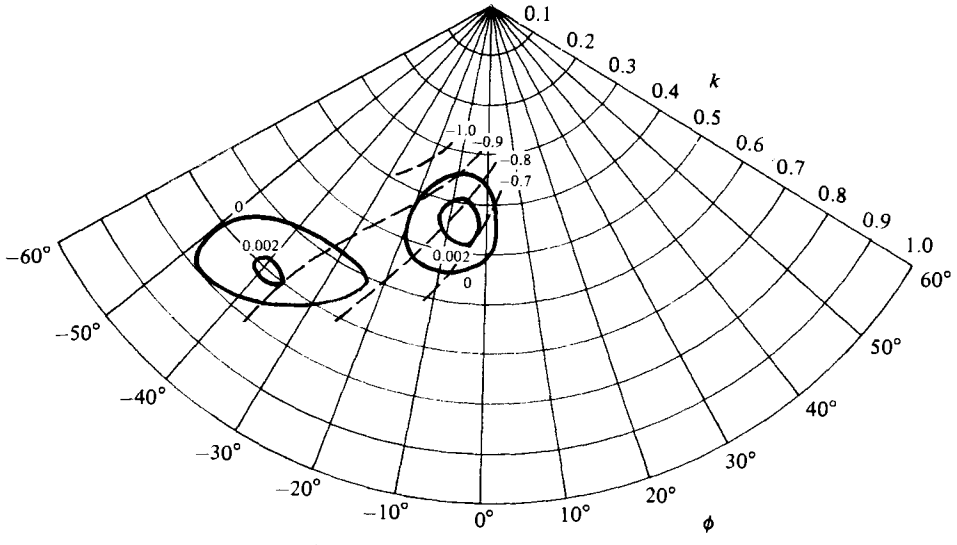

FIGURE 4. Same as figure 2 except $M = 8$ and $Re = 65$.

figure 4). These modes have phase velocities of order unity, large negative angles or orientation, and wavenumbers that are larger than the ones for class A type instability. Henceforth, this mode will be referred to as class C type instability. In fact, the presence of this mode can also be inferred from figure 2, but at that Mach number it is subdominant to the class A type instability. For the Mach-number and Reynolds-number combination corresponding to figure 4, only class A and class C type modes are present. As the Mach number is increased, the growth rates for class A modes becomes larger than the ones for class C modes, and also class B type instability occurs (see figure 5). In fact, extensive numerical calculations were carried out to verify that the class A and B modes reported here are modified A and B type waves for the homogeneous fluid case and that the class C mode is not related to those.

Critical Reynolds numbers for the different instability modes for air at room

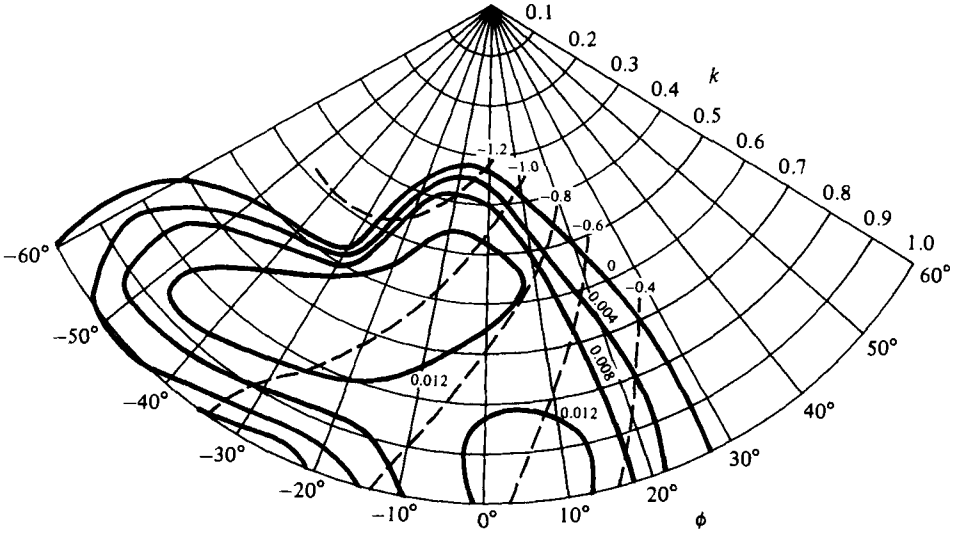

FIGURE 5. Same as figure 2 except $M = 12$ and $Re = 65$.

temperature have been calculated, and these are shown in table 1 as functions of the Mach number. The critical Reynolds number for the class A type instability increases with the Mach number up to a Mach number of about five. Thereafter, the class A modes are destabilized by further increases in the Mach number. The class B and class C type instabilities are continuously destabilized by the effects of compressibility. Note that for a Mach number of 12, the class C type modes are the first to become unstable.

4. Summary

Class A waves are primarily caused by an interaction of the shear force associated with the azimuthal velocity component and the Coriolis force (Greenspan 1968). For moderate values of the Mach number, the compressibility and the heat conduction of the gas tend to increase the critical Reynolds number for class A type instability. For sufficiently large values of the Mach number, however, further increase of the Mach number leads to a destabilization of these waves. For air at room temperature, this change occurs for a Mach number of about five.

The class B type instability is essentially an inviscid inflectional instability associated with the radial velocity distribution (Greenspan 1968). As the Mach number is increased, the critical Reynolds number for this type of instability is decreased. The class B waves are destabilized by the effects of compressibility and heat conduction.

A new mode of instability, that does not have a counterpart in the homogeneous-fluid case, has been found to occur for finite values of the Mach number. These instability waves, labelled class C, have high phase velocities and large negative angles of orientation. These instability modes would be clearly distinguishable from the other two modes in an experiment. An increase in the Mach number leads to further destabilization of these waves.

Appendix. Gas centrifuge application

A technologically important application for the analysis presented here is the stability of Ekman-layer flow in gas centrifuges for uranium enrichment. The low densities that are likely to occur in the vicinity of the axis of rotation in such a device has two effects. The mean free path of the molecules will become large, and the thickness of the Ekman layer will increase in that region.

For the continuum hypothesis to hold, the Knudsen number must be very small, i.e.

$$Kn \equiv \lambda/L \ll 1, \tag{A 1}$$

where λ is the mean free path and L is a characteristic lengthscale of the continuum flow field. The mean free path can be calculated using the kinetic theory of dilute gases, i.e. by assuming that the gas is in local equilibrium and that the particle velocity distribution is a Maxwellian distribution centred on the local continuum velocity. The details of such a calculation can be found in Huang (1963, p. 93). Apart from a multiplicative factor of order unity, one finds

$$\lambda \approx \frac{m}{\rho^* \pi a^2}, \tag{A 2}$$

where m is the molecular weight and a is the collisional diameter of the molecules. The continuum lengthscale of interest here is the Ekman layer thickness, i.e.

$$L = \left(\frac{\mu}{\rho^* \Omega}\right)^{\frac{1}{2}}. \tag{A 3}$$

By using the kinetic theory of dilute gases, the dynamic shear viscosity can be estimated (again disregarding a multiplicative factor of order unity) as

$$\mu \approx \rho^* c \lambda, \tag{A 4}$$

(Huang 1963, p. 109), where $c = (\gamma R T^*)^{\frac{1}{2}}$ is the adiabatic speed of sound. Combination of (2.7d), (A 1), (A 3) and (A 4) gives the following criterion for the validity of the continuum assumption:

$$\left(\frac{\lambda M}{r_0^*}\right)^{\frac{1}{2}} \ll 1. \tag{A 5}$$

The left-hand side of this inequality can be rewritten as

$$\left(\frac{\lambda M}{r_0^*}\right)^{\frac{1}{2}} = \left(\frac{\lambda_p M_p}{r_p^*}\right)^{\frac{1}{2}} \exp\left\{\frac{\gamma M_p^2}{4}\left[\left(\frac{r_p^*}{r_0^*}\right)^2 - 1\right]\right\}, \tag{A 6}$$

where the subscript p denotes variables evaluated at the periphery. As can be seen from (A 6), the left-hand side of (A 5) can change an order of magnitude across the radial extent of the centrifuge, even for moderate values of the Mach number. Presumably, rarified flow will occur in the vicinity of the axis of rotation. The stability analysis, which is local, is then only valid for larger radii. The effects of rarified flow are usually, even if somewhat incorrectly, ignored in theoretical investigations of the gas centrifuge (e.g. Sakurai & Matsuda 1974). In addition to the inequality (A 5), the Ekman layer must be a boundary layer in the usual sense. This is ensured if the local Ekman number (cf. (2.10a)) is, as assumed here, vanishingly small.

REFERENCES

BATCHELOR, G. K. 1970 *An Introduction to Fluid Dynamics*. Cambridge University Press.

CALDWELL, D. R. & VAN ATTA, C. W. 1970 Characteristics of Ekman boundary layer instabilities. *J. Fluid Mech.* **44**, 79.

FALLER, A. J. 1963 An experimental study of the instability of the laminar Ekman boundary layer. *J. Fluid Mech.* **15**, 560.

FALLER, A. J. & KAYLOR, R. E. 1966 A numerical study of the instability of the laminar Ekman boundary layer. *J. Atmos. Sci.* **23**, 53.

GANS, R. F. 1974 On the Poincare problem for a compressible medium. *J. Fluid Mech.* **62**, 657.

GANS, R. F. 1975 On the stability of shear flows in a rotating gas. *J. Fluid Mech.* **68**, 403.

GREENSPAN, H. P. 1968 *The Theory of Rotating Fluids*, 2nd edn. Cambridge University Press.

GUSEV, A. & BARK, F. H. 1980 Stability of rotation-modified plane Poisseuille flow. *Phys. Fluids* **23**, 2171.

HUANG, K. 1963 *Statistical Mechanics*. Wiley.

HULTGREN, L. S. 1978 Stability of axisymmetric gas flows in a rapidly rotating cylindrical container. Ph.D. thesis, Department of Aeronautics and Astronautics, Massachusetts Institute of Technology.

LALAS, D. P. 1975 The 'Richardson' criterion for compressible swirling flows. *J. Fluid Mech.* **69**, 65.

LILLY, D. K. 1966 On the instability of the Ekman boundary layer. *J. Atmos. Sci.* **23**, 481.

LIN, C. C. 1966 *The Theory of Hydrodynamic Stability*. Cambridge University Press.

MILES, J. W. 1981 Waves in a rapidly rotating gas. *J. Fluid Mech.* **107**, 487.

MOBERG, H. 1979 Diploma thesis, Department of Mechanics, Royal Institute of Technology, Stockholm, Sweden (in Swedish).

MORTON, J. B. & SHAUGHNESSY, E. J. 1972 Waves in a gas in solid-body rotation. *J. Fluid Mech.* **56**, 277.

NIELSEN, H. B. & TRUE, H. 1978 Numerical solution of the nonlinear stability of an incompressible Ekman layer. In *Numer. Meth. – 6th Intl Conf., Tblisi, USSR, 21–24 June.*

SAKURAI, T. & MATSUDA, T. 1974 Gasdynamics of a centrifugal machine. *J. Fluid Mech.* **62**, 727.

SPALL, J. R. & WOOD, H. G. 1984 An analysis of the stability of the compressible Ekman boundary layer. *Phys. Fluids* (to be published).

SPOONER, G. F. 1982 Continuous temporal eigenvalue spectrum of an Ekman boundary layer. *Phys. Fluids* **25**, 1958.

SPOONER, G. F. & CRIMINALE, W. O. 1982 The evolution of disturbances in an Ekman boundary layer. *J. Fluid Mech.* **115**, 327.

TATRO, P. R. & MOLLO-CHRISTENSEN, E. L. 1967 Experiments on Ekman layer instability. *J. Fluid Mech.* **28**, 531.

WARREN, F. H. 1975 A comment on Gans' stability criterion for steady inviscid helical gas flows. *J. Fluid Mech.* **68**, 413.